CHAPTER 5 ELECTRON DRIVEN PROCESSES FOR AQUA DNA CONSTITUENTS

"This chapter presents calculated CSs for various electron driven processes with hydrated DNA nucleobases (adenine, thymine, guanine, cytosine, and uracil). Employing the SCOP, CSP-ic, and novel 2p-SEM formalisms to determine cross sections relevant for assessing DNA damage induced by electron impact. We estimated the dielectric constant (ε) of hydrated nucleobases and analyzed correlations between total scattering CSs, molecular properties (Z and α), and ionization CSs with α and ε. These results enhance understanding of electron-induced processes in biological systems and support modeling of radiation damage in DNA".

5.1Introduction

The application of ionizing radiation is a fundamental practice in medical research and healthcare. It is extensively utilized not only as a powerful therapeutic tool, particularly in cancer treatments like radiotherapy, but also as a critical probe in radio diagnostic techniques, including imaging modalities such as X-rays, CT scans, and PET scans. These dual roles highlight its versatility and importance in both diagnosing and treating various medical conditions. While traditional beliefs attributed the majority of extremely energetic radiation damage to biological tissue to ballistic impact, it is now recognized that secondary species resulting from primary ionization play a significant role in radiation damage [1]. The primary ionizing particles deposit the majority of their energy in the aqueous medium through various interaction, such as excitations and ionizations. This substantial energy transfer releases numerous secondary electrons, which, in turn, interact with various biological substances, leading to radiation damage. DNA/RNA molecules are particularly sensitive to such radiation among all living tissues, experiencing various types of damage [2] induced by exposure to radiations, including those caused by secondary species such as electrons.

To effectively understand and predict the location and extent of biological cell damage caused by radiation, it is crucial to model the tracks of both primary as well as secondary species as they traverse a biological medium. Charged-particle track structures depict the path taken by these particles through the medium, offering insights into the radiation's impact [3]. Stochastic simulations rely on cross-section values to model the full range of interactions between primary and secondary species at the atomic or molecular scale. Therefore, the precision of these CSs is essential to ensure the reliability of the simulations.

To date, a considerable amount of the CSs data has been documented about the interaction of electrons with DNA/RNA constituents in its gaseous state [4–8]. While, the CSs for interaction processes in the condensed phase are available, their scope is limited to energies below 20 eV [9,10]. A more accurate representation of DNA's behavior can be achieved by examining its interactions within an aqueous environment, where it forms hydrogen bonds [11,12] with water molecules. This contrasts with theoretical models that consider DNA in isolated gaseous or condensed states. This has prompted us to take up the investigation of interactions of electrons with aqueous DNA nucleobases.

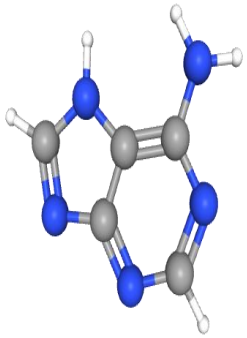

$C_5H_5N_5$ (Adenine)

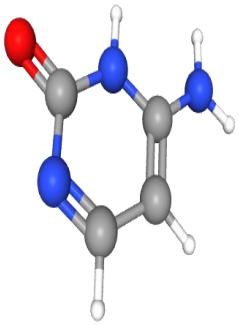

$C_4H_5N_3O$ (Cytosine)

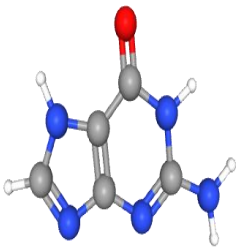

$C_5H_5N_5O$ (Guanine)

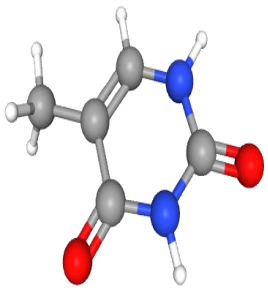

$C_5H_6N_2O_2$ (Thymine)

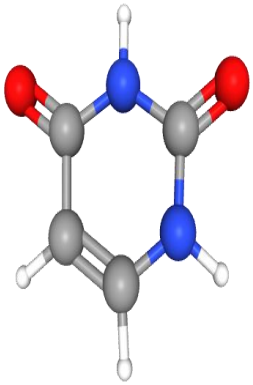

$C_4H_4N_2O_2$ (Uracil)

Figure 5.1 Chemical structure of studied DNA/RNA nucleobases

This study focuses on electron collisions with aqua DNA nucleobases. We calculated varieties of CSs i.e. ionization, inelastic, total and elastic, in an aqueous environment. Notably, this is the first investigation of electron-induced processes in aqueous DNA components, covering energies from the IP to 5000 eV. A schematic representation of the present molecules has been shown in Figure 5.1.

5.2 A group of DNA/RNA nucleobases in aqueous environment

This section provides a comprehensive analysis of the elastic and inelastic collisions involving aqueous biomolecules, specifically Adenine, Guanine, Cytosine, Thymine, and Uracil. These interactions are explored in detail to understand their behavior and impact in an aqueous environment, focusing on their relevance to electron-induced processes and their role in biological systems.

5.2.1 Prior work and molecular properties

A comprehensive review is provided in the current study, detailing the impact energy ranges, various cross-sections (CSs), phases, and methodologies employed by researchers for the investigated targets in Table 5.1.

Table 5.1 Priore work on aqua DNA/RNA bases

Qty.	Phase	E_i range (eV)	Method	Ref.
Q_{inel}	Molecules in water	20-10,000	Dielectric response theory	Tan and coworkers [13]
Q_{ion}	Condensed phase	10-500		Tan and coworkers [14]
Q_{ion}		1-10,000		Vera and coworkers [15]

The molecular properties of the DNA/RNA nucleobases are tabulated in Table 5.2 and it is used for computation of cross sections data.

Table 5.2 Molecular properties in of the DNA/RNA nucleobases aqueous environment

DNA/RNA bases	IP (eV) [16,17]	E_{gap} (eV)
$C_5H_5N_5$	5.00	5.25 [18]
$C_5H_6N_2O_2$	5.40	5.20 [21]
$C_5H_5N_5O$	4.80	4.80 [20]
$C_4H_5N_3O$	5.50	5.35 [17]
$C_4H_4N_2O_2$	5.55	5.70 [19]

5.3 Results for DNA constituents in aqua phase

This section presents an in-depth analysis of electron impact cross-sections for aqueous DNA/RNA bases over wide energy range spectrum from IP to 5 keV. Three computational approaches—2p-SEM, SCOP, CSP-ic, and—are employed to establish correlations that estimate correlation to calculate dielectric constant (ε) and dipole polarizability (α). These findings provide valuable insights into the interaction characteristics of biomolecules in aqueous environments.

(i) Inelastic processes:

Through figures 5.2, 5.4, 5.6, 5.8 and 5.10, inelastic effect for the studied aqueous DNA constituents are presented as a function of electron energy, alongside existing experimental and theoretical findings [13–15].

(ii) Elastic processes:

Figures 5.3, 5.5, 5.7, 5.9, and 5.11 display the elastic and inelastic cross-sections for aqueous DNA constituents as a function of incident electron energies ranging from the molecular IP to 5000 eV. The obtained results show excellent matching with available findings, thereby validating the 2p-SEM for the more complex molecules whose atomic number (Z) lies between 55<Z<95. This supports the effectiveness of the recently developed 2p-SEM approach.

5.3.1 Adenine ($C_5H_5N_5$)

The inelastic processes for adenine are shown in figure 5.2.

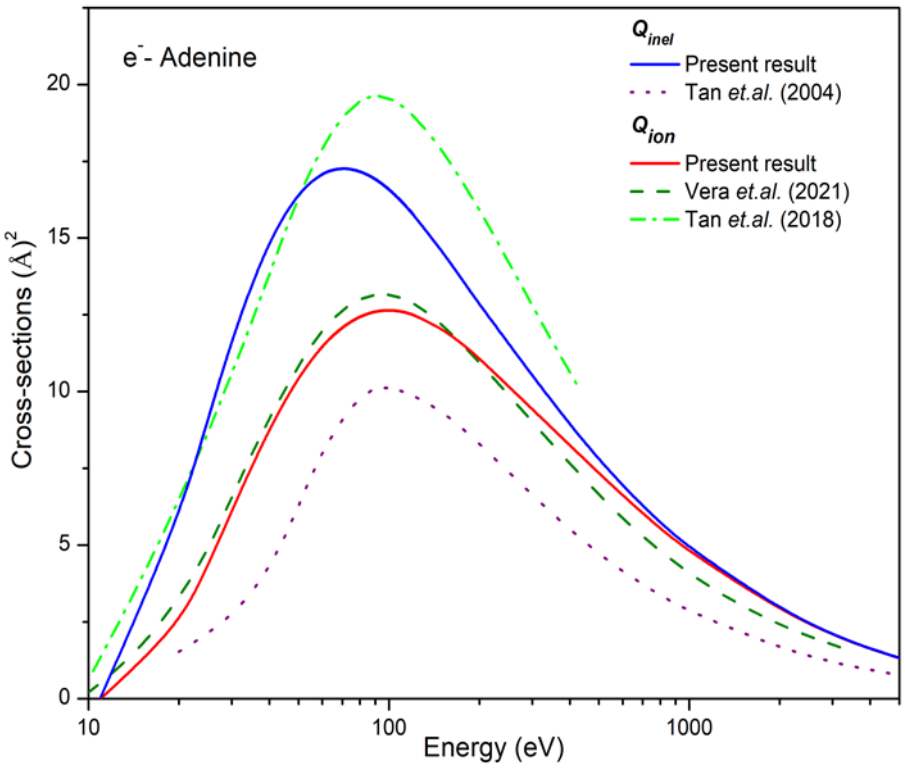

Figure 5.2 Q_{inel} and Q_{ion} CSs for Adenine

Q_{inel}:- solid blue: Present; dotted curve: Tan and coworkers [13]; Q_{ion}:- solid red: Present; dash Dot curve: Tan and coworkers[14]; dashed curve: Vera and coworkers [15];

The top most curve represent total inelastic cross sections, Q_{inel}. Tan and coworkers [13] have reported the data of Q_{inel} for DNA bases in condensed phase using dielectric response theory. However, their Q_{inel} underestimate present calculated data and its lower values than Q_{ion} [14].

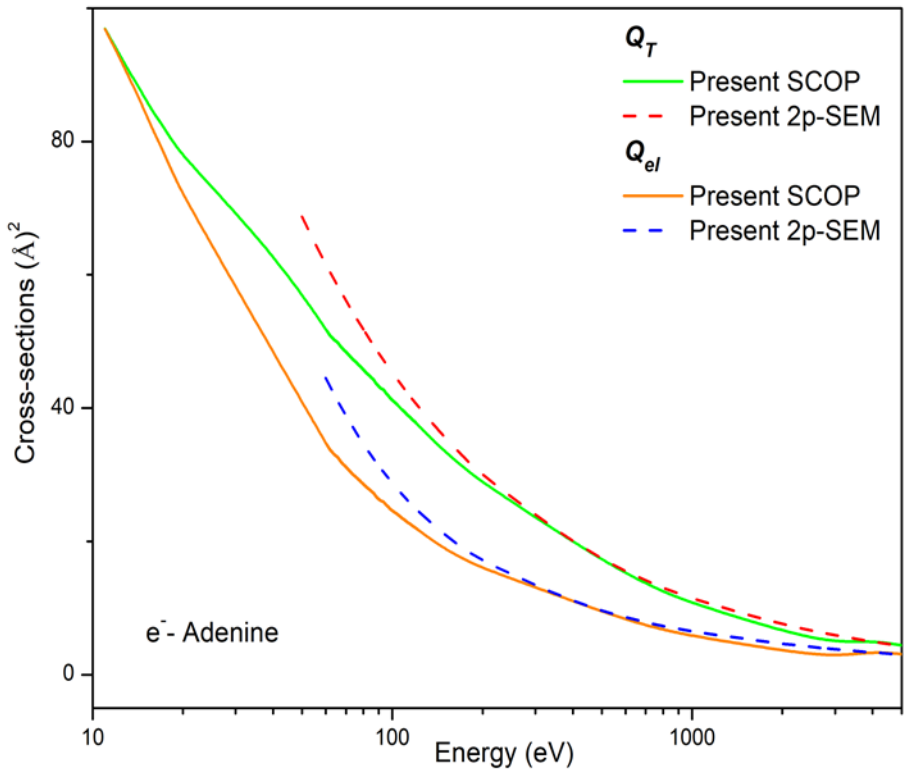

Figure 5.3 Q_{el} and Q_T for Adenine

Q_T(SCOP):- Solid green; dash red: Q_T(2p-SEM); Q_{el}(SCOP):- solid orange; dashed blue:- Q_{el}(2p-SEM)

Figure 5.3, illustrates elastic and total CSs for adenine. These results are obtained through 2p-SEM over the energy from 50-5000 eV and shows good agreement with present SCOP formalism. The calculated total CSs values for Adenine are shown in table 5.3.

Table 5.3 CSs data (Å^2) for Adenine

E_i (eV)	Q_{ion}	Q_{el}	Q_T
11	0.00	96.82	96.88
20	2.35	72.02	77.85
40	8.76	48.42	63.27
60	11.46	34.79	51.86

70	12.08	31.17	48.43
80	12.43	28.59	45.76
90	12.60	26.34	43.26
100	12.65	24.60	41.18
200	11.09	15.98	28.83
400	8.25	11.04	19.91
600	6.61	8.24	15.16
800	5.54	6.74	12.47
1000	4.79	5.81	10.72
2000	2.89	3.61	6.53
3000	2.07	2.69	4.78
4000	1.62	3.48	5.11
5000	1.33	3.07	4.40

5.3.2 Guanine ($C_5H_5N_5O$)

For *e*-guanine, the inelastic CSs and available data are displayed in Figure 5.4.

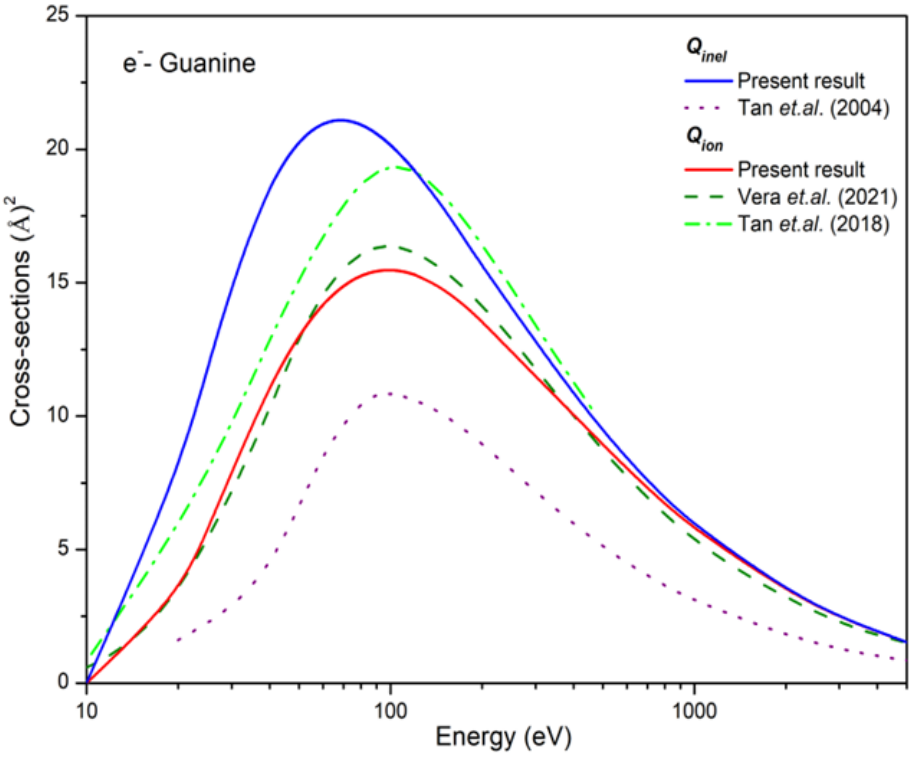

Figure 5.4 Q_{inel} and Q_{ion} for Guanine

Q_{inel}:- solid blue: present ; dotted: Tan and coworkers [13]; Q_{ion}:- solid red: present; dashed curve: Vera and coworkers [15]; dash dot: Tan and coworkers [14]

The upper curves in the graph represent the complete inelastic cross-sections (Q_{inel}). Authors [13] utilized dielectric theory along with Penn's theorem to report Q_{inel} data for DNA in an aqueous environment. Figure 5.5 compares elastic and total CSs for DNA in aqueous state, calculated via 2p-SEM and SCOP methods. The figure provides a comparison of these cross-sections, showcasing the results derived from both methods and highlighting their consistency or discrepancies for the examine range of incident energy.

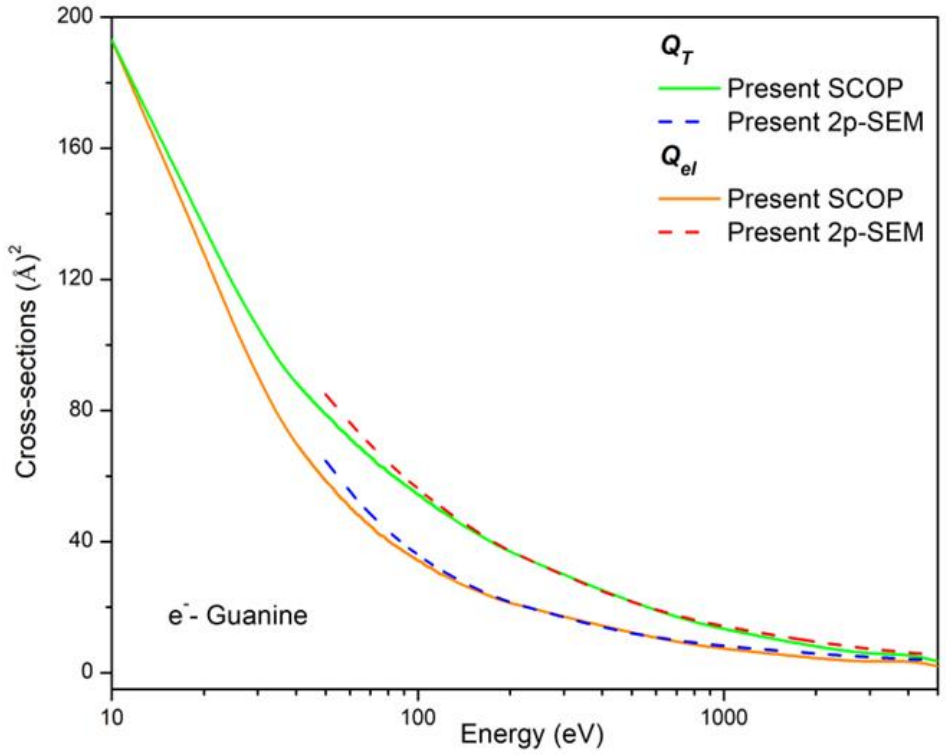

Figure 5.5* Q_{el} and Q_T *for Guanine

Q_T:- solid green: SCOP; red dashed: 2p-SEM; Q_{el}:- solid orange: Present; dashed blue: 2p-SEM

The calculated total CSs data are shown in table 5.4 for Guanine.

Table 5.4 CSs data (Å²) for Guanine

E_i (eV)	Q_{ion}	Q_{el}	Q_T
10	0.00	192.95	192.95
20	3.27	128.23	136.08
30	7.90	90.45	105.29
40	11.04	70.00	88.51
50	12.99	58.51	78.76

60	14.17	50.40	71.35
70	14.87	44.76	65.84
80	15.25	40.28	61.20
90	15.43	36.98	57.56
100	15.47	34.26	54.41
200	13.56	21.22	36.86
400	10.04	14.30	25.07
600	8.02	10.59	18.98
800	6.71	8.56	15.48
1000	5.78	7.34	13.27
2000	3.46	4.38	7.87
3000	2.48	3.17	5.66
4000	1.93	3.83	5.77
5000	1.53	2.00	3.54

5.3.3 Cytosine ($C_4H_5N_3O$)

The present Q_{inel} and Q_{ion} with **t**he available comparisons are shown in below figure 5.6.

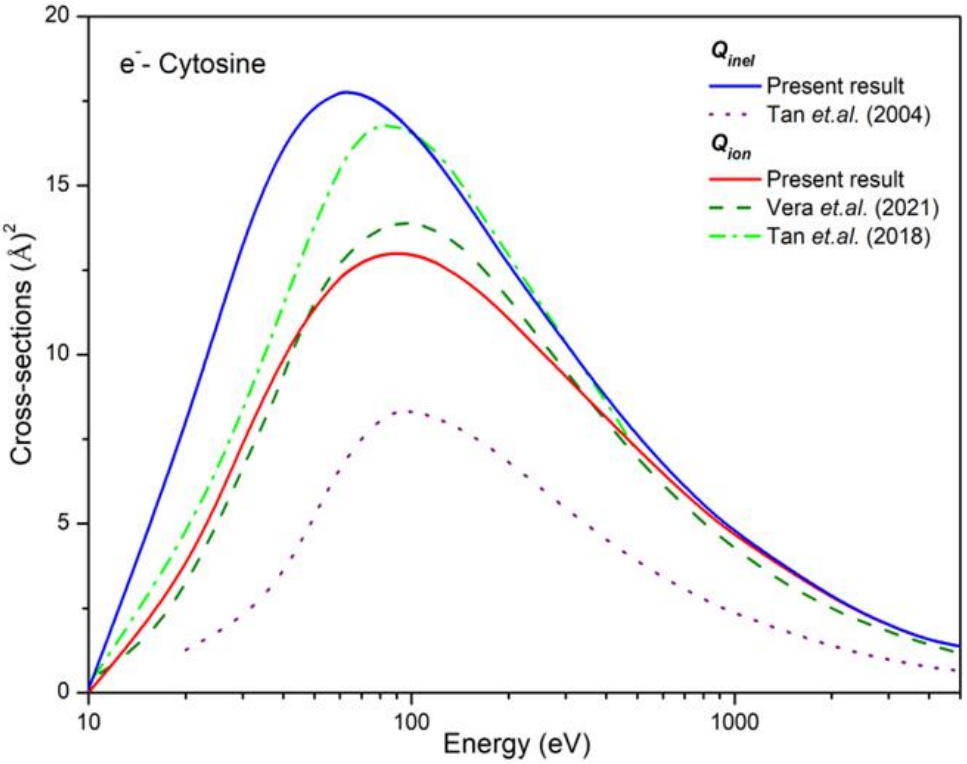

Figure 5.6 Q_{inel} and Q_{ion} for Cytosine

Q_{inel}:- solid blue: present; dotted: Tan and coworkers [13]; Q_{ion}:- solid red: Present; dashed: Vera and coworkers [15]; dash dot: Tan and coworkers [14]

An equivalent unit of DNA molecule was dissolved in water, containing a 50:50 ratio of Adenine-Thymine and Guanine-Cytosine base pairs. This DNA molecule was then separated into its five constituent bases.

In figure 5.7, the elastic and total CSs calculated using 2p-SEM and SCOP are displayed. The results show excellent agreement across the entire energy range, demonstrating the consistency of the two approaches.

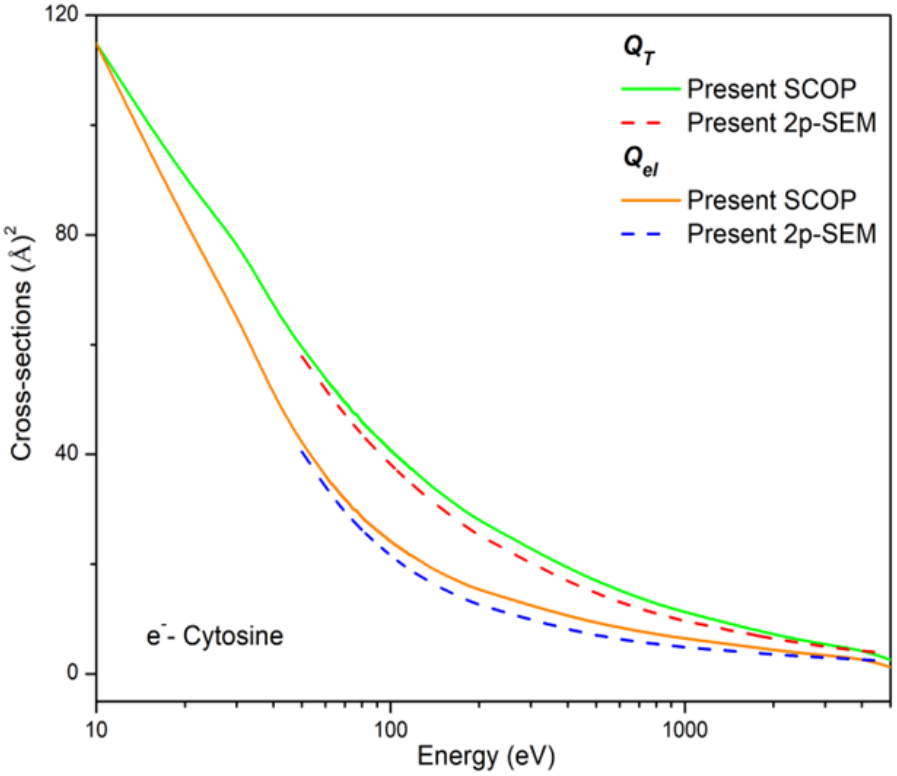

Figure 5.7 Q_{el} and Q_T for Cytosine

Q_T:- solid green: SCOP; red dashed: 2p-SEM; Q_{el}:- solid orange: Present; dashed blue: 2p-SEM

The calculated total CSs values are displayed in table 5.5 for *e*-Cytosine.

Table 5.5 Total CSs (Å²) for Cytosine

E_i (eV)	Q_{ion}	Q_{el}	Q_T
10	0.01	114.81	114.92
20	3.42	82.11	89.88
30	7.42	65.54	79.04
40	9.94	50.70	66.94
50	11.42	42.01	59.40

60	12.26	36.26	54.00
70	12.71	31.81	49.49
80	12.93	28.52	45.93
90	12.99	26.11	43.14
100	12.95	24.15	40.75
200	11.07	15.32	27.96
400	8.13	10.45	19.12
600	6.47	8.42	15.16
800	5.40	7.23	12.78
1000	4.64	6.46	11.21
2000	2.77	4.33	7.13
3000	1.98	3.35	5.34
4000	1.55	2.80	4.35
5000	1.37	1.23	2.60

5.3.4 Thymine ($C_5H_6N_2O_2$)

The present results of Q_{ion} and Q_{inel} are shown in figure 5.8.

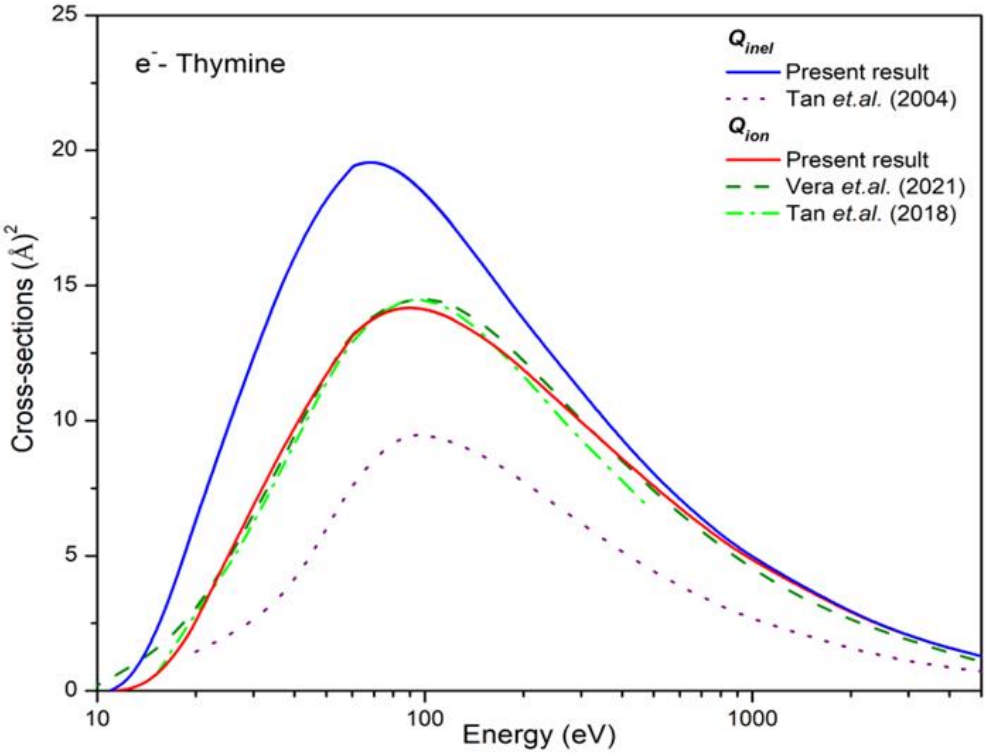

Figure 5.8 Q_{inel} and Q_{ion} for Thymine

Q_{inel}:- Solid blue: Present; dotted: Tan and coworkers [13]; Q_{ion}:- Solid red: Present; dashed: Vera and coworkers [15]; dash dot: Tan and coworkers [14]

The current Q_{ion} agrees well with previous comparisons across the entire energy range. Authors, [14,15] have previously reported the Q_{ion} data for aqua DNA bases through the dielectric theory. The present Q_{ion} are found reasonably good with the data of Vera and coworkers [15].

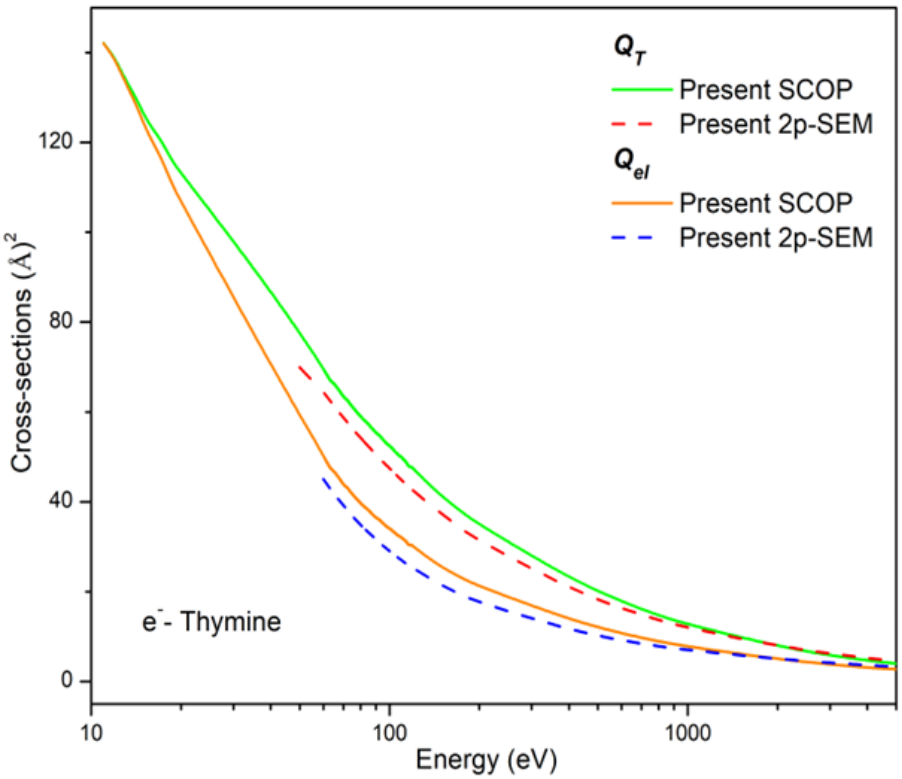

Figure 5.9* Q_{el} and Q_T *for Thymine

Q_T:- solid green: SCOP; red dashed: 2p-SEM; Q_{el}:- solid orange: Present; dashed blue: 2p-SEM

Figure 5.9 illustrates the elastic (Q_{el}) and total (Q_T) CSs obtained through "SCOP" and "2p-SEM" techniques. The results exhibit a strong agreement across the entire energy spectrum, highlighting the reliability of both methods. The calculated total CSs values are displayed in Table 5.6 for *e*-Thymine.

Table 5.6 Total CSs (Å^2) for Thymine

E_i (eV)	Q_{ion}	Q_{el}	Q_T
11	0.00	142.10	142.12
20	2.55	106.87	113.23
40	10.01	70.34	87.17

60	13.13	50.41	69.81
70	13.79	43.97	63.52
80	14.09	39.72	59.05
90	14.17	36.54	55.44
100	14.12	34.05	52.44
200	11.91	21.23	34.96
400	8.58	13.73	22.93
600	6.76	10.71	17.77
800	5.60	8.88	14.67
1000	4.81	7.74	12.66
2000	2.84	4.95	7.82
3000	2.03	3.78	5.82
4000	1.57	3.10	4.68
5000	1.29	2.69	3.98

5.3.5 Uracil ($C_4H_4N_2O_2$)

The present results of Q_{ion} and Q_{inel} for uracil are shown in figure 5.10.

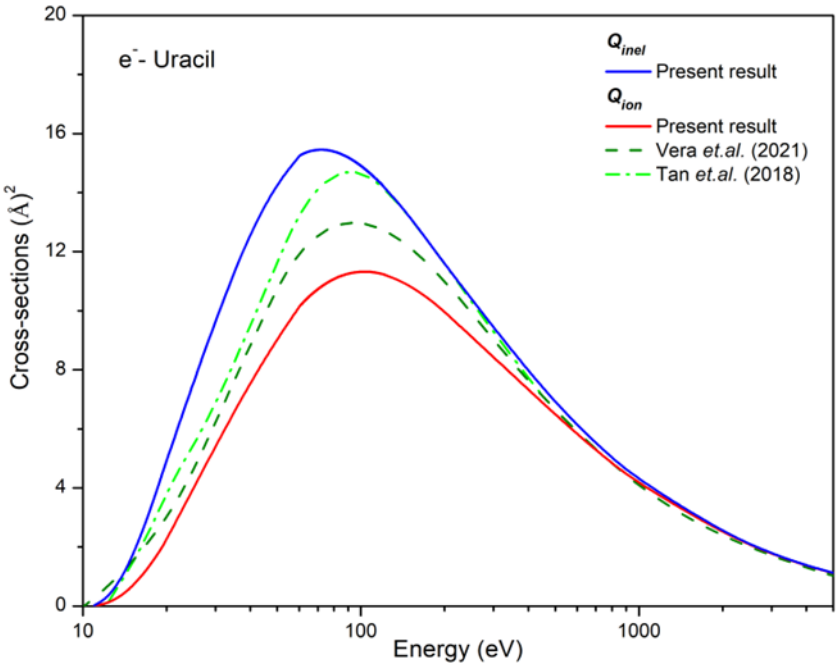

Figure 5.10 Q_{inel} and Q_{ion} for Uracil

Q_{inel}:- Solid blue: Present; Q_{ion}:- solid red: Present; dashed: Vera and coworkers [15]; dash dot: Tan and coworkers [14]

As can be seen, the ionization cross-sections reported by Tan and coworker [14] are consistently higher than both the present data and those of Vera and coworker [15]. The observed discrepancy may be attributed to use of various material phases in the current study. Figure 5.11 presents the Q_{el} and Q_T CSs computed using the SCOP and 2p-SEM methods. Both approaches demonstrate strong complementarity and consistent agreement across the entire energy spectrum, reinforcing the reliability of the results.

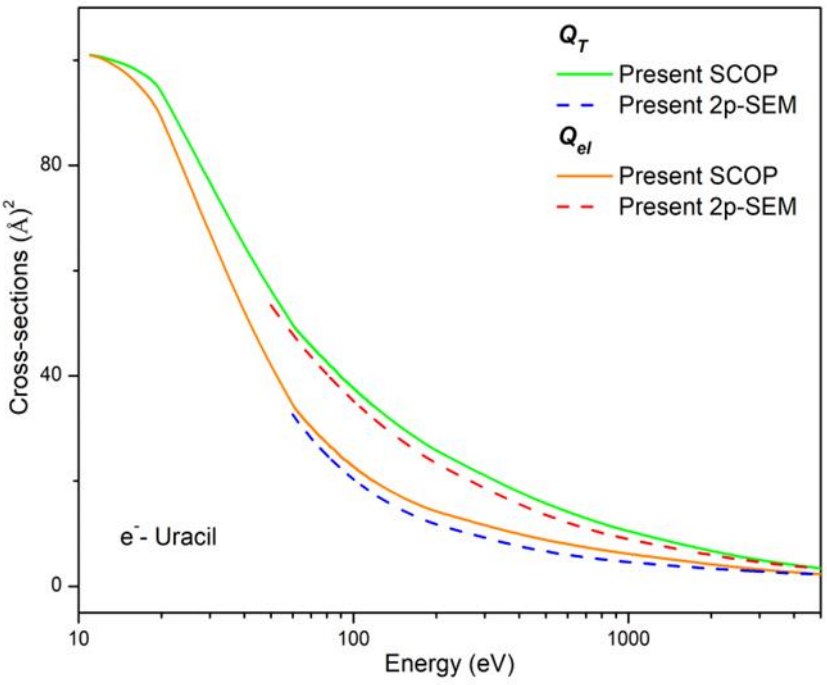

Figure 5.11* Q_{el} and Q_T *for Uracil

Q_T(SCOP):-solid green; red dashed: Q_T (2p-SEM); Q_{el}(SCOP):- solid orange; dashed blue: Q_{el} (2p-SEM)

The computed aggregate CSs values are presented in Table 5.7 for e-Uracil.

Table 5.7 Total CSs data (Å^2) for Uracil

E_i (eV)	Q_{ion}	Q_{el}	Q_T
11	0.01	100.96	100.99
20	2.24	89.44	94.39
40	7.69	50.97	64.10
60	10.14	34.53	49.79
70	10.73	30.30	45.75
80	11.08	27.23	42.62

90	11.26	24.62	39.81
100	11.32	22.71	37.62
200	9.97	14.15	25.73
400	7.33	9.78	17.69
600	5.81	8.00	14.11
800	4.83	6.90	11.91
1000	4.15	6.14	10.42
2000	2.46	4.13	6.62
3000	1.76	3.20	4.98
4000	1.37	2.66	4.03
5000	1.12	2.31	3.43

5.4 Correlation study

Using the calculated ionization CSs (Q_{ion}), key molecular properties, including dielectric constant (ε) and polarizability (α), were derived for aqueous DNA bases. The correlation study plays a crucial role in linking these cross-sections with molecular properties, offering a deeper understanding of the interaction mechanisms and behavior of DNA bases in aqueous environments. Such insights are vital for applications in biophysics, radiation biology, and molecular modeling.

5.4.1 Polarizability (α)

In accordance with Harland [22] was proposed qualitative relationship between the maximum ionization CSs and polarizability (α),

$$Q_{ion(\max)} = \frac{e}{4\varepsilon_o}\sqrt{\frac{\alpha}{\Delta}} \tag{5.1}$$

Harland proposed that in the gaseous phase of a molecular system, the Δ is equivalent to the ionization potential (IP). However, for the present work involving aqua compounds, Δ is the sum of IP and E_{gap}. Ionization channel opens when the incident energy exceeds the threshold value, where $\Delta = IP + E_{gap}$.

We have predicted the values of α as given in the table 5.8 for the present studied molecules through equation 5.1.

Table 5.8 Predicted polarizability α (Å)^3

Molecule	**Δ (eV)**	**Max.Q_{ion} (Å)^2**	**α (Å)^3**	
			Predicted	***Ref.*** [23]
$C_5H_5N_5$	10.26	12.64	11.55	14.34
$C_5H_5N_5O$	9.59	15.46	16.18	15.27
$C_5H_6N_2O_2$	10.59	14.16	14.98	13.36
$C_4H_5N_3O$	10.86	12.98	12.87	11.48
$C_4H_4N_2O_2$	11.26	11.33	10.14	10.40

As shown in Table 5.8, the calculated polarizabilities (α) align well with those reported by Nakagawa [23] for condensed DNA molecules.

5.4.2 Dielectric constant (ε)

In this work, two mathematical equations for the dielectric constant (ε) were obtained through the Max.Q_{ion} on α and ε, as presented in equation 2.79 and 2.80 (chapter 2). The first equation of ε as a function of Max.Q_{ion}, was derived by integrating the relationship between Max.Q_{ion} with α.

The expression of Clausius Mosotti,

$$\frac{\varepsilon-1}{\varepsilon+2} = C \cdot (Max.Q_{ion})^2 N\Delta \qquad (5.2)$$

The value of constant C is equal to $\frac{64\pi}{3}\left(\frac{\varepsilon_o}{e}\right)^2$ and the number density is denoted as N.

The Onsager [24] dielectric representation, which is highly effective for describing liquids, is expressed as:

$$\frac{\varepsilon-1}{\varepsilon+2} = \frac{4\pi}{3}\alpha N + \frac{(\varepsilon-\varepsilon_{\infty})(2\varepsilon+\varepsilon_{\infty})}{\varepsilon(\varepsilon_{\infty}+2)^2} \tag{5.3}$$

This expression is believed to be more suitable for the current study of aqueous DNA constituents. Additionally, we propose an equation for the dielectric constant as a function of $Q_{ion(m)}$, given by

$$\frac{\varepsilon-1}{\varepsilon+2} = C \cdot \left(Q_{ion(m)}\right)^2 N\Delta + \frac{(\varepsilon-\varepsilon_{\infty})(2\varepsilon+\varepsilon_{\infty})}{\varepsilon(\varepsilon_{\infty}+2)^2} \tag{5.4}$$

Here, ε_{∞} represents the dielectric constant at high frequencies.

Table 5.9 Calculated ε

Target	**Max.Q_{ion} (Å)^2**	**Dielectric constant (ε)**		
		Eq. 5.2	**Eq. 5.4**	**Ref.** [25]
$\mathbf{C_5H_5N_5}$	12.64	2.23	1.01	1.59
$\mathbf{C_5H_5N_5O}$	15.46	3.24	0.86	1.77
$\mathbf{C_5H_6N_2O_2}$	14.16	3.40	1.00	1.59
$\mathbf{C_4H_5N_3O}$	12.98	2.85	1.04	1.71
$\mathbf{C_4H_4N_2O_2}$	11.33	2.30	0.99	-

As shown in table 5.9, the values of ε is calculated using equation 5.4 and matches well with those reported by Szarek [25].

5.5 Chapter summary

This chapter reported the aqueous phase of DNA, investigating various molecular processes triggered by electron collisions. Considering the prevalence of hydrogen bonds in DNA, this approach provides a more accurate representation of its behaviour in biological systems. To comprehensively assess “Radiation-induced damage” to DNA, including “single and double-strand breaks”, it is essential to study inelastic electron interactions with aqueous DNA.

The current work quantifies various interaction processes occurring during electron impact on DNA constituents in aqueous phase. The current study also examines the dependence of Q_T on impact energy and molecular properties, leading to the proposal of a novel approach called 2p-SEM, for calculating Q_T, which represents the initial endeavor to present a cohesive equation for Q_T, suitable for extensive and intricate molecular systems comprising 55 to 95 electrons, across an energy spectrum of 50-5000 eV. By examining the relationship between molecular ionization and, we have computed target dielectric constant and polarizability. The dielectric constant is determined from the Q_{ion} using both the C. M. and Onsager approaches (equations 5.2 and 5.4). Our calculated results are compared with existing one. In the lack of previous studies on aqua DNA molecules, this investigation of several cross-sections and the calculation of dielectric constant, polarizability etc. are extremely useful.

5.6 Bibliography

[1] B. Boudaïffa, P. Cloutier, D. Hunting, M. A. Huels, and L. Sanche, *Cross Sections for Low-Energy (10-50 eV) Electron Damage to DNA*, Radiat Res **157**, 227 (2002).

[2] H. Nikjoo, R. Taleei, T. Liamsuwan, D. Liljequist, and D. Emfietzoglou, *Perspectives in Radiation Biophysics: From Radiation Track Structure Simulation to Mechanistic Models of DNA Damage and Repair*, Radiation Physics and Chemistry **128**, 3 (2016).

[3] D. T. Goodhead, *Initial Events in the Cellular Effects of Ionizing Radiations: Clustered Damage in DNA*, Int J Radiat Biol **65**, 7 (1994).

[4] P. Mozejko, and L. Sanche, *Cross Sections for Electron Scattering from Selected Components of DNA and RNA*, Radiation Physics and Chemistry **73**, 77 (2005).

[5] J. N. Bull, J. W. L. Lee, and C. Vallance, *Absolute Electron Total Ionization Cross-Sections: Molecular Analogues of DNA and RNA Nucleobase and Sugar Constituents*, Physical Chemistry Chemical Physics **16**, 10743 (2014).

[6] C. J. Colyer, S. M. Bellm, F. Blanco, G. Garcia, and B. Lohmann, *Elastic Electron Scattering from the DNA Bases Cytosine and Thymine*, Phys Rev A **84**, 042707 (2011).

[7] S. Mokrani, H. Aouchiche, and C. Champion, *Elastic Scattering of Electrons by DNA Bases*, Radiation Physics and Chemistry **172**, 108735 (2020).

[8] M. Vinodkumar and C. Limbachiya, *Electron Impact Total and Ionization Cross-Sections for DNA Based Compounds*, Mol Phys **111**, 215 (2013).

[9] L. Toburen, *Ionization and Charge-Transfer: Basic Data for Track Structure Calculations*, Radiat Environ Biophys **37**, 221 (1998).

[10] A. Bass and L. Sanche, *Absolute and Effective Cross-Sections for Low-Energy Electron-Scattering Processes within Condensed Matter*, Radiat Environ Biophys **37**, 243 (1998).

[11] H. Khesbak, O. Savchuk, S. Tsushima, and K. Fahmy, *The Role of Water H-Bond Imbalances in B-DNA Substate Transitions and Peptide Recognition Revealed by Time-Resolved FTIR Spectroscopy*, J Am Chem Soc **133**, 5834 (2011).

[12] Helmholtz Association of German Research Centres, *Water Molecules Characterize the Structure of DNA Genetic Material.*, https://www.sciencedaily.com/releases/2011/04/110426091122.htm#citation_apa.

[13] Z. Tan, Y. Xia, X. Liu, M. Zhao, Y. Ji, F. Li, and B. Huang, *Cross Sections of Electron Inelastic Interactions in DNA*, Radiat Environ Biophys **43**, 173 (2004).

[14] P. De Vera, I. Abril, and R. Garcia-Molina, *Excitation and Ionisation Cross-Sections in Condensed-Phase Biomaterials by Electrons down to Very Low Energy: Application to Liquid Water and Genetic Building Blocks*, Physical Chemistry Chemical Physics **23**, 5079 (2021).

[15] H. Q. Tan, Z. Mi, and A. A. Bettiol, *Simple and Universal Model for Electron-Impact Ionization of Complex Biomolecules*, Phys Rev E **97**, 1 (2018).

[16] C. E. Crespo-Hernández, R. Arce, Y. Ishikawa, L. Gorb, J. Leszczynski, and D. M. Close, *Ab Initio Ionization Energy Thresholds of DNA and RNA Bases in Gas Phase and in Aqueous Solution*, Journal of Physical Chemistry A **108**, 6373 (2004).

[17] H. Fernando, G. A. Papadantonakis, N. S. Kim, and P. R. Lebreton, *Conduction-Band-Edge Ionization Thresholds of DNA Components in Aqueous Solution*, Proc Natl Acad Sci U S A **95**, 5550 (1998).

[18] S. Gop, R. Sutradhar, S. Chakraborty, and T. P. Sinha, *The Study of Energetic and Electronic Properties of Metal-Adenine Complex in Solvent Phase: A Density Functional Theory Approach*, in *AIP Conference Proceedings*, Vol. 2162 (American Institute of Physics Inc., 2019).

[19] M. T. Baei, M. R. Taghartapeh, E. T. Lemeski, and A. Soltani, *A Computational Study of Adenine, Uracil, and Cytosine Adsorption upon AlN and BN Nano-Cages*, Physica B Condens Matter **444**, 6 (2014).

[20] R. di Felice, A. Calzolari, E. Molinari, and A. Garbesi, *Ab Initio Study of Model Guanine Assemblies: The Role of (Formula Presented) Coupling and Band Transport*, Phys Rev B Condens Matter Mater Phys **65**, 1 (2002).

[21] J. MacNaughton, A. Moewes, and E. Z. Kurmaev, *Electronic Structure of the Nucleobases*, Journal of Physical Chemistry B **109**, 7749 (2005).

[22] P. W. Harland and C. Vallance, *Ionization Cross-Sections and Ionization Efficiency Curves from Polarizability Volumes and Ionization Potentials*, Int J Mass Spectrom Ion Process **171**, 173 (1997).

[23] S. Nakagawa, *Polarizable Model Potential Function for Nucleic Acid Bases*, J Comput Chem **28**, 1538 (2007).

[24] L. Onsager, *Electric Moments of Molecules in Liquids*, J Am Chem Soc **58**, 1486 (1936).

[25] P. Szarek, *Electric Permittivity in Individual Atomic and Molecular Systems Through Direct Associations with Electric Dipole Polarizability and Chemical Hardness*, Journal of Physical Chemistry C **121**, 12593 (2017).